Chapter 7 Diffraction from distorted crystallites

In this chapter, diffraction from crystallites including **structural defects** is discussed. Structural defects should always exist in realistic materials, even though it may sometimes be very few, and no significant effects might be observed. Actually, the effects of structural defects on the observed diffraction measurements is quite significant in some cases. Detailed analysis of observed diffraction peak profile provides information about the structural defects, and it is often important for evaluation of practical materials. For example, hardening of metals generally causes structural defects, and the hardness and brittleness are strongly affected by the structural defects.

It should be noted that there are various kinds of structural defects, and it is often a very complicated problem how to describe the structural defects. At first, the structural defects are classified into three groups based on the viewpoint of **dimensionality**.

(i) **Point defect** : **zero-dimensional** structural defects. It includes "**vacancy**" that means absence of atoms that should exists at a location, "**interstitial**" that means existence of atoms where it should not exist in the regular structure, and "**substitutional solid solution**" that means substitution of an atom by another element. Figure 7.1 schematically illustrates the three types of point defects.

(ii) **Linear defect** : **one-dimensional** structural defects, including "**dislocation**". There are two types of dislocations: one is "**screw-type dislocation**" and the other is "**edge-type dislocation**". Figure 7.2 schematically illustrates the two types of dislocations.

(iii) **Planar defect** : **two-dimensional** structural defects, including "**stacking fault**". The "**surface**", "**interface**" or "**grain-boundary**" may also be classified into the two-dimensional structural defects.

In principle, point defects can cause distortion of the crystal structure, but no significant effects on peak profile are practically observed, probably because the deformation caused by the point defects is not coherent, and the effect is similar to the random variation in the atomic positions caused by thermal vibration. But the average interplanar spacing is slightly changed by the point defects or impurity atoms, and it is empirically known that the change in the unit cell volume or dimension of the crystal is proportional to the concentration of impurity, which is called the **Vegard's law**.

The effects of linear and planar structural defects are naturally anisotropic, and they often coexist in a deformed crystal. The anisotropic effects of dislocation may be modelled through the elastic deformation around the defects, but omitted in this text. A simplified model about strain (though it may not be realistic...) and a model for stacking fault are introduced in this chapter.
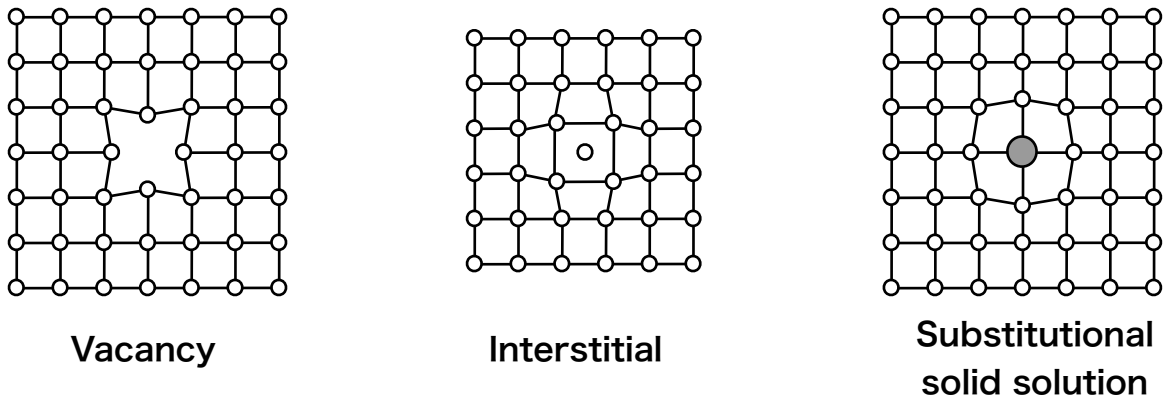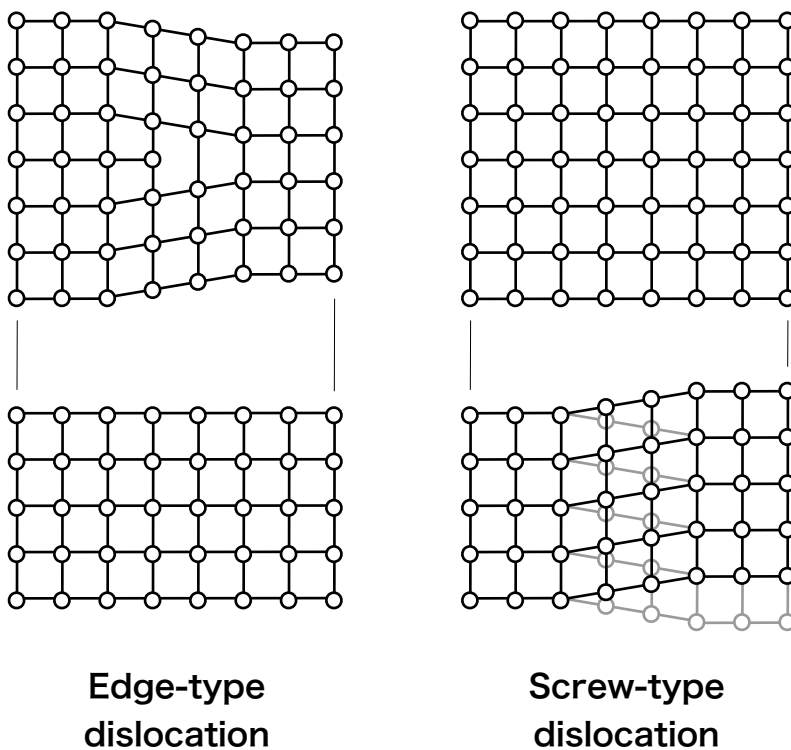
Fig. 7.1 Point defects

Fig. 7.2 Dislocations

7-1 Most simple model for strain

The simplest model for the effects of structural defects on diffraction peak profile is introduced in this section. We assume that the lattice constants or the values of interplanar spacings are not constant, but are varied on different region in a specimen. It is likely to be caused by inhomogeneous chemical composition or internal stress caused by misfit at grain boundary in polycrystalline materials.

Note that compressive stress should reduce the interplanar spacings along the direction of the force, and tensile stress should expand the interplanar spacings. The technique to evaluate the macroscopic internal stress from the observed amount of the X-ray diffraction peak shift is called

"**residual stress measurement**", though it is rather a "residual strain measurement" combined with the speculation of stress based on the known elastic properties of the material.

When the statistical distribution of the interplanar distance d_{hkl}, or the reciprocal interplanar distance d_{hkl}^*, is modeled by the normal distribution, the probability density function about the relative deviation of the interplanar spacing :

$$\varepsilon = \frac{\Delta d_{hkl}}{d_{hkl}} \sim \frac{\Delta d_{hkl}^*}{d_{hkl}^*} \tag{7.1}$$

should be given by a common formula :

$$f(\varepsilon) = \frac{1}{\sqrt{2\pi}\sigma} e^{-\frac{\varepsilon^2}{2\sigma^2}}, \tag{7.2}$$

where σ can definitely be related to the "root mean square of the relative strain".

By differentiating the Bragg's equation :

$$d^* = \frac{2\sin\theta}{\lambda}, \tag{7.3}$$

we have the following formula,

$$\Delta d^* = \frac{\cos\theta}{\lambda}(\Delta 2\theta), \tag{7.4}$$

and the following relation between the relative deviation of the interplanar distance ε and the deviation of the diffraction angle $\Delta 2\theta$,

$$(\Delta 2\theta) = \frac{2\Delta d^* \tan\theta}{d^*} = 2\varepsilon \tan\theta. \tag{7.5}$$

Then, the root mean square of the deviation in the diffraction angle is given by

$$\sqrt{\left\langle (\Delta 2\theta)^2 \right\rangle} = 2\sqrt{\left\langle \varepsilon^2 \right\rangle}\tan\theta = 2\sigma\tan\theta. \tag{7.6}$$

Note that the broadening of the diffraction peak profile caused by the strain should be proportional to $\tan\theta$ on the scale of 2θ.

On the other hand, the broadening caused by the finite size of crystallites should be proportional to $1/\cos\theta$, as shown in the Scherrer's equation. If the total broadening of the observed diffraction peak profile is expressed by the sum of the effects of finite size and strain, it should be expressed by

$$\Delta 2\theta = X/\cos\theta + Y\tan\theta, \tag{7.7}$$

where X and Y are proportionality factors. By multiplying Eq. (7.7) by $\cos\theta$, we have

$$(\Delta 2\theta)\cos\theta = X + Y\sin\theta. \tag{7.8}$$

So it is expected that the y-section (X) will give the size effect, and the slope (Y) will give the strain effect, when the plot of $(\Delta 2\theta)\cos\theta$ against $\sin\theta$ lies on a common line. This plot is called

"**Williamson-Hall plot**", and it is often claimed that the size and strain effects can be separated by this method, called as "**Williamson-Hall method**". An example of an idealistic Williamson-Hall plot is shown in Fig. 7.3.
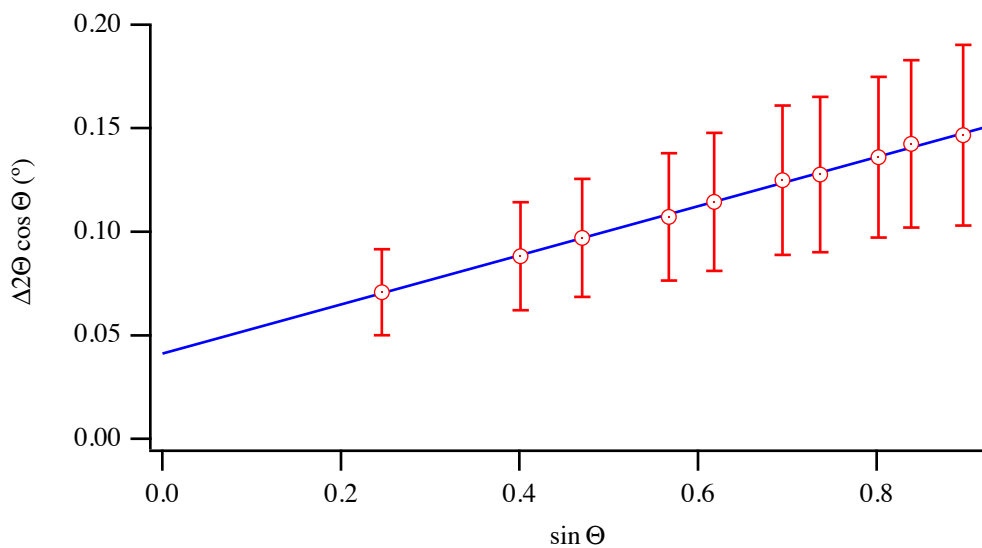
Fig. 7.3 Williamson-Hall plot (for isotropic broadening).

The amount of strain $\sqrt{\langle \varepsilon^2 \rangle}$ evaluated by the above method is often called "**microstrain**" or "**inhomogeneous strain**".

The strain in a crystal should be anisotropic, when the stress caused by a linear defect (dislocation) is dominant. For example, in the case of the edge-type dislocation including linear defects along the [100]-direction, the interplanar spacing of (h00) planes will be less affected, while the spacing of the lattice planes having the normal direction perpendicular to the [100]-direction should be most strongly affected by the distortion. It is possible that h00-reflections are less broadened, while the broadening about $0kl$-reflections are more significant. The **crystal habit** caused by anisotropic crystal growth may also cause size-broadening depending on the orientation of the crystal structure. The author would like to note that anisotropic line broadening is often observed in realistic materials.

When the broadening of diffraction peaks is anisotropic, the Williamson-Hall plot will not lie on a common linear dependence, but we may possibly find what kind of anisotropy exists from the Williamson-Hall plot, provided that the Miller indices are attached to each data point. It is often recommended to attach the Miller indices to the data points in the Williamson-Hall plot, which is called "**indexed Williamson-Hall plot**". You may sometimes find a linear relation about $100, 200,$ 300-reflections and another linear relation about $111, 222, 333$-reflections, for example.

7-2 Paterson's theory for stacking fault

In a cubic close packing structure, triangular arrangement of atomic planes are stacking in the pattern of $\cdots ABCABCABC \cdots$. It is likely that the stacking scheme is ocasionally broken and shows such a pattern : (i) $\cdots ABCA\underline{B}ABCABC \cdots$, or (ii) $\cdots ABCAB\underline{C}BACBA \cdots$. The stacking fault of type (i) can be caused by deformation by the stress along opposite directions on the top and bottom faces parallel to the (111)-plane, for example, (shear deformation), and called "**deformation fault**". The stacking fault of the type (ii) may appear in the growth process of the crystal, and is called "**growth fault**" or "**twin fault**".

In the following, the Paterson's theory for diffraction peak profile affected by the deformation fault is described. (A theory for growth fault has also been proposed, but it may be less convincing as compared with the theory for deformation fault.)

7-2-1 Calculation of diffraction peak profile affected by deformation fault

Assume the lattice vectors of the cubic close packing structure to be $\vec{a}$, $\vec{b}$, $\vec{c}$, and the lattice constant to be a. The vectors $\vec{a}$, $\vec{b}$, $\vec{c}$ have the common length of a , and orthogonal to each other. As we are interested in the stacking fault along the (111)-direction, a hexagonal system having the c-axis parallel to the (111)-direction of the cubic system is introduced.

The lattice vectors of the hexagonal system are defined by the following equations,

$$\vec{a}_{\mathrm{H}} = -\vec{a} + \vec{b} \tag{7.9}$$

$$\vec{b}_{\mathrm{H}} = -\vec{b} + \vec{c} \tag{7.10}$$

$$\vec{c}_{\mathrm{H}} = \vec{a} + \vec{b} + \vec{c} \tag{7.11}$$

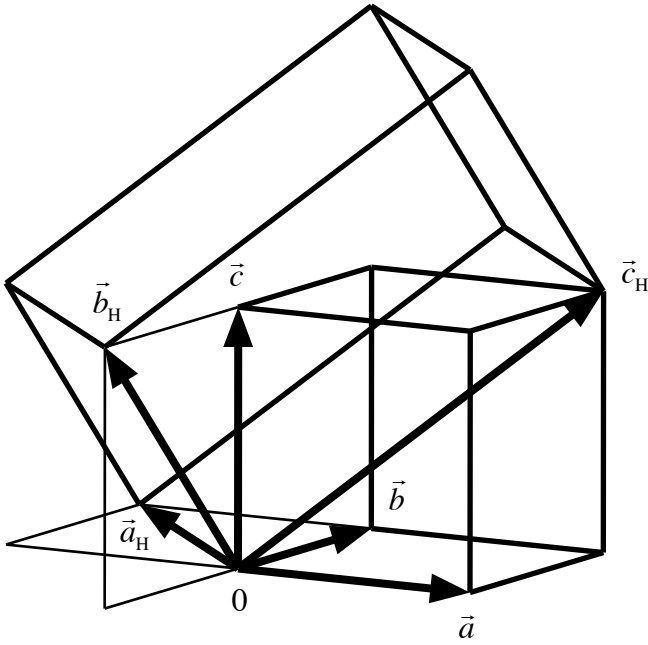The relationship between the cubic and hexagonal lattice vectors are shown in Fig. 7.4.

Fig. 7.4 Cubic and hexagonal lattice vectors.

The volume of the hexagonal cell is calculated by applying the relation :

$$\vec{a}_{\mathrm{H}} \times \vec{b}_{\mathrm{H}} = \left(-\vec{a} + \vec{b} \right) \times \left(-\vec{b} + \vec{c} \right)$$

$$= \vec{a} \times \vec{b} - \vec{a} \times \vec{c} - \vec{b} \times \vec{b} + \vec{b} \times \vec{c}$$

$$= a \left(\vec{a} + \vec{b} + \vec{c} \right), \tag{7.12}$$

which gives

$$V_{\mathrm{H}} = \left(\vec{a}_{\mathrm{H}} \times \vec{b}_{\mathrm{H}} \right) \cdot \vec{c}_{\mathrm{H}} = a \left(\vec{a} + \vec{b} + \vec{c} \right) \cdot \left(\vec{a} + \vec{b} + \vec{c} \right) = 3a^{3} . \tag{7.13}$$

And the reciprocal lattice vectors for the hexagonal lattice are given by

$$\vec{a}_H^* = \frac{\vec{b}_H \times \vec{c}_H}{V_H} = \frac{\left(-\vec{b}+\vec{c}\right)\times\left(\vec{a}+\vec{b}+\vec{c}\right)}{3a^3}$$

$$= \frac{\vec{c}-\vec{a}+\vec{b}-\vec{a}}{3a^2} = \frac{-2\vec{a}+\vec{b}+\vec{c}}{3a^2} , \tag{7.14}$$

$$\vec{b}_H^* = \frac{\vec{c}_H \times \vec{a}_H}{V_H} = \frac{\left(\vec{a}+\vec{b}+\vec{c}\right)\times\left(-\vec{a}+\vec{b}\right)}{3a^3}$$

$$= \frac{\vec{c}-\vec{b}+\vec{c}-\vec{a}}{3a^2} = \frac{-\vec{a}-\vec{b}+2\vec{c}}{3a^2} , \tag{7.15}$$

$$\vec{c}_H^* = \frac{\vec{a}_H \times \vec{b}_H}{V_H} = \frac{\vec{a}+\vec{b}+\vec{c}}{3a^2} . \tag{7.16}$$
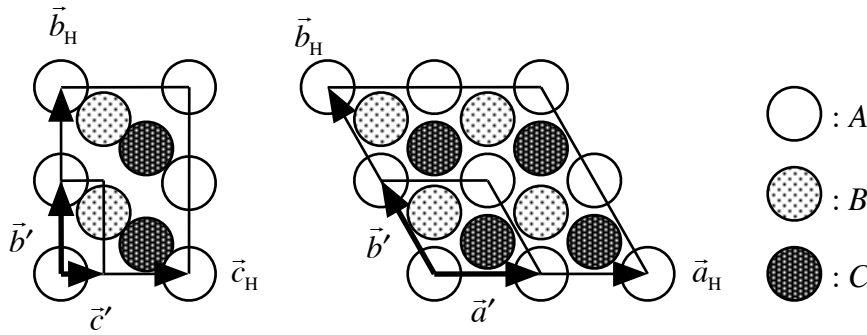

Fig. 7.5 Arrangement of atoms in the cubic close packing structure and the hexagonal cell.

The hexagonal unit cell is divided into a smaller cell defined by $\vec{a}' = \vec{a}_H / 2$, $\vec{b}' = \vec{b}_H / 2$, $\vec{c}' = \vec{c}_H / 3$, as shown in Fig. 7.5. Note that the cell defined by $\vec{a}'$, $\vec{b}'$ and $\vec{c}'$ is not a unit structure, but it may simplify the calculation of the intensity, because the number of atoms in the cell is unity. The volume of the small hexagonal cell is given by

$$V' = \frac{a^3}{4} ,$$

and the reciprocal lattice vectors are given by

$$\vec{a}'^* = \frac{\vec{b}' \times \vec{c}'}{V'} = \frac{2\left(-2\vec{a}+\vec{b}+\vec{c}\right)}{3a^3} ,$$

$$\vec{b}'^* = \frac{\vec{c}' \times \vec{a}'}{V'} = \frac{2\left(-\vec{a}-\vec{b}+2\vec{c}\right)}{3a^3} ,$$

$$\vec{c}'^* = \frac{\vec{a}' \times \vec{b}'}{V'} = \frac{\vec{a}+\vec{b}+\vec{c}}{a^2} .$$

The total diffraction intensity from a crystal should be given by

$$I(\vec{K}) = \sum_{\xi,\eta,\varsigma} \sum_{\xi',\eta',\varsigma'} F_{\xi,\eta,\varsigma}(\vec{K}) F_{\xi',\eta',\varsigma'}^*(\vec{K}) \exp\left\{2\pi i \vec{K} \cdot \left[(\xi-\xi')\vec{a}' + (\eta-\eta')\vec{b}' + (\varsigma-\varsigma')\vec{c}'\right]\right\},$$

$$\tag{7.17}$$

where $F_{\xi,\eta,\varsigma}(\vec{K})$ is the structure factor located at the position : $\xi\vec{a}' + \eta\vec{b}' + \varsigma\vec{c}'$. Since the number

of atoms included in the cell is always one, the absolute value of $F_{\xi,\eta,\varsigma}(\vec{K})$ should be independent

of the location of the cell, but the phase of the structure factor varies on the atomic position in this small hexagonal cell.

　Here we assume that the scattering vector is expressed by

$$\vec{K} = h'\vec{a}'^* + k'\vec{b}'^* + l'\vec{c}'^* ,$$ (7.18)

and the values of h' , k' , l' can have fractional values (not restricted to integer values). Then the diffraction intensity should be given by

$$I(\vec{K}) = \sum_{\xi,\eta,\varsigma}\sum_{\xi'',\eta'',\varsigma''} F_{\xi,\eta,\varsigma}(\vec{K})F^*_{\xi+\xi'',\eta+\eta'',\varsigma+\varsigma''}(\vec{K})\exp\left[2\pi\,i\,\vec{K}\cdot\left(\xi''\vec{a}' + \eta''\vec{b}' + \varsigma''\vec{c}'\right)\right]$$

$$= \sum_{\xi,\eta,\varsigma}\sum_{\xi'',\eta'',\varsigma''} F_{\xi,\eta,\varsigma}(\vec{K})F^*_{\xi+\xi'',\eta+\eta'',\varsigma+\varsigma''}(\vec{K})\exp\left[2\pi\,i\left(h'\xi'' + k'\eta'' + l'\varsigma''\right)\right] ,$$ (7.19)

for $\xi' = \xi + \xi''$, $\eta' = \eta + \eta''$, $\varsigma' = \varsigma + \varsigma''$, and the above equation is rewritten as

$$I(\vec{K}) = \sum_{\xi''=-\infty}^{\infty}\sum_{\eta''=-\infty}^{\infty}\sum_{\varsigma''=-\infty}^{\infty} V_{\xi'',\eta'',\varsigma''}J_{\xi'',\eta'',\varsigma''}(\vec{K})\exp\left[2\pi\,i\left(h'\xi'' + k'\eta'' + l'\varsigma''\right)\right] ,$$ (7.20)

where $J_{\xi'',\eta'',\varsigma''}(\vec{K})$ is defined by

$$J_{\xi'',\eta'',\varsigma''}(\vec{K}) \equiv \sum_{\xi,\eta,\varsigma} F_{\xi,\eta,\varsigma}(\vec{K})F^*_{\xi+\xi'',\eta+\eta'',\varsigma+\varsigma''}(\vec{K}) .$$ (7.21)

The value of $V_{\xi'',\eta'',\varsigma''}$ in Eq. (7.20) represents "the fraction of existence of translation vector

$\xi''\vec{a}' + \eta''\vec{b}' + \varsigma''\vec{c}'$ in the crystal". The value should be close to unity for small value of

$\left|\xi''\vec{a}' + \eta''\vec{b}' + \varsigma''\vec{c}'\right|$, but generally becomes smaller for larger values of $\left|\xi''\vec{a}' + \eta''\vec{b}' + \varsigma''\vec{c}'\right|$, because

the translation symmetry is not satisfied beyond the size of the crystal. Here we introduce a further assumption that the crystal is sufficiently large and the value of $V_{\xi'',\eta'',\varsigma''}$ is always equal to 1.

　Even if there exist stacking faults in the crystal, the atomic arrangement in one atomic layer should still be the triangular lattice for the close packing structure. Since the relative arrangement of atoms among the one-atom layer is the same, the structure factor $F_{\xi,\eta,\varsigma}(\vec{K})$ for the common value

of ς should be equivalent, that is, the relation :

$$F_{\xi,\eta,\varsigma}(\vec{K}) = F_{\xi+\xi'',\eta+\eta'',\varsigma}(\vec{K}) ,$$

which means the translational symmetry along the two dimensional atomic layer, is always satisfied. Then the value of $J_{\xi'',\eta'',\varsigma''}(\vec{K})$ is also independent of ξ'' and η'' , and it varies only on

the value of ς'' . Therefore, we can ignore the subscripts ξ'' and η'' , and assume

$J_{\xi'',\eta'',\varsigma''}(\vec{K}) = J_{\varsigma''}(\vec{K})$.

　Eq. (7.20) can then be rewritten as

$$I(h',k',l') = \sum_{\xi''=-\infty}^{\infty} e^{2\pi i h' \xi''} \sum_{\eta''=-\infty}^{\infty} e^{2\pi i k' \eta''} \sum_{\varsigma''=-\infty}^{\infty} J_{\varsigma''}(h',k',l') e^{2\pi i l' \varsigma''}. \tag{7.22}$$

The intensity $I(h',k',l')$ has non-zero values only for the case both h' and k' are integer, because

$\displaystyle\sum_{\xi''=-\infty}^{\infty} e^{2\pi i h' \xi''} = 0$ and $\displaystyle\sum_{\eta''=-\infty}^{\infty} e^{2\pi i k' \eta''} = 0$ for non-integer values of h' and k'. Now, we can assume that

$$I(h',k',l') = \sum_{m=-\infty}^{\infty} J_m(h',k',l') e^{2\pi i m l'} \quad (h',\ k' : \text{integer}), \tag{7.23}$$

without loss of generality. Note that non-integer value of l' is still allowed here.

Let us consider the three types of atomic layers, A, B and C. With respect to the atomic later A, the layer B is displaced by $\dfrac{\vec{a}' + 2\vec{b}'}{3}$, and the layer C is displaced by $\dfrac{2\vec{a}' + \vec{b}'}{3}$, as can be seen in Fig. 7.5. Then the structure factors of the A, B, C layers are given by

$$F_A(\vec{K}) = F_0(\vec{K}), \tag{7.24}$$

$$F_B(\vec{K}) = F_0(\vec{K}) \exp\left[2\pi i \vec{K} \cdot \left(\frac{\vec{a}' + 2\vec{b}'}{3} \right) \right], \tag{7.25}$$

$$F_C(\vec{K}) = F_0(\vec{K}) \exp\left[2\pi i \vec{K} \cdot \left(\frac{2\vec{a}' + \vec{b}'}{3} \right) \right]. \tag{7.26}$$

Here, we define the probabilities that two layers separated by m layers satisfying the relations $A \cdots A$, $A \cdots B$ and $A \cdots C$ to be P_m^0, P_m^+ and P_m^-, respectively. Of course, the relation :

$$P_m^0 + P_m^+ + P_m^- = 1 \tag{7.27}$$

should always be satisfied. Then the expectation value of $J_m(\vec{K})$ is given by

$$\begin{aligned}
\langle J_m(\vec{K}) \rangle = \frac{1}{3} \Big[&F_A(\vec{K}) F_A^*(\vec{K}) P_m^0 + F_A(\vec{K}) F_B^*(\vec{K}) P_m^+ + F_A(\vec{K}) F_C^*(\vec{K}) P_m^- \\
&+ F_B(\vec{K}) F_B^*(\vec{K}) P_m^0 + F_B(\vec{K}) F_C^*(\vec{K}) P_m^+ + F_B(\vec{K}) F_A^*(\vec{K}) P_m^- \\
&+ F_C(\vec{K}) F_C^*(\vec{K}) P_m^0 + F_C(\vec{K}) F_A^*(\vec{K}) P_m^+ + F_C(\vec{K}) F_B^*(\vec{K}) P_m^- \Big],
\end{aligned} \tag{7.28}$$

and substitution of $F_A(\vec{K})$, $F_B(\vec{K})$, $F_C(\vec{K})$ by the expressions in Eqs. (7.24)-(7.26) will give

$$\begin{aligned}
\langle J_m(\vec{K}) \rangle = \frac{1}{3} |F_0(\vec{K})|^2 \Big\{ &P_m^0 + \exp\left[-\frac{2\pi i(h' + 2k')}{3} \right] P_m^+ + \exp\left[-\frac{2\pi i(2h' + k')}{3} \right] P_m^- \\
&+ P_m^0 + \exp\left[\frac{2\pi i(-h' + k')}{3} \right] P_m^+ + \exp\left[\frac{2\pi i(h' + 2k')}{3} \right] P_m^- \\
&+ P_m^0 + \exp\left[\frac{2\pi i(2h' + k')}{3} \right] P_m^+ + \exp\left[\frac{2\pi i(h' - k')}{3} \right] P_m^- \Big\} \\
= \frac{1}{3} |F_0(\vec{K})|^2 \Big\{ &P_m^0 + \exp\left[\frac{2\pi i(-h' + k')}{3} \right] P_m^+ + \exp\left[\frac{2\pi i(h' - k')}{3} \right] P_m^-
\end{aligned}$$

$$+ P_m^0 + \exp\left[\frac{2\pi i(-h'+k')}{3}\right] P_m^+ + \exp\left[\frac{2\pi i(h'-k')}{3}\right] P_m^-$$

$$+ P_m^0 + \exp\left[\frac{2\pi i(-h'+k')}{3}\right] P_m^+ + \exp\left[\frac{2\pi i(h'-k')}{3}\right] P_m^- \biggr\}.$$

Finally, we obtain the result :

$$\left\langle J_m(\vec{K}) \right\rangle = \left| F_0(\vec{K}) \right|^2 \left[P_m^0 + P_m^+ e^{-2\pi i(h'-k')/3} + P_m^- e^{2\pi i(h'-k')/3} \right]. \tag{7.29}$$

In the following, the formula to express the probability P_m^0, P_m^+, P_m^- by the probability of appearance of deformation fault α will be derived.

First, let us evaluate the the probability P_m^0. It is assumed that the zero-th layer belongs to the type-A layer. Possible 4 patterns, where the m-th layer also belongs to the type-A layer, are following,

0		$m-2$	$m-1$	m
A	$\cdots$	A	B	A
A	$\cdots$	A	C	A
A	$\cdots$	B	C	A
A	$\cdots$	C	B	A

The possibility for "B next to A", "C next to B" and "A next to C" are all given by $(1-\alpha)$, (regular arrangement), while the possibility for "C next to A", "A next to B" and "B next to C" are all given by α (false arrangement). Therefore,

$$P_m^0 = P_{m-2}^0 (1-\alpha)\alpha + P_{m-2}^0 \alpha(1-\alpha) + P_{m-2}^+ (1-\alpha)(1-\alpha) + P_{m-2}^- \alpha\alpha, \tag{7.30}$$

and the following relations :

$$P_{m-1}^0 = P_{m-2}^+ \alpha + P_{m-2}^- (1-\alpha), \tag{7.31}$$

$$P_{m-2}^0 + P_{m-2}^+ + P_{m-2}^- = 1 \tag{7.32}$$

are satisfied. From the above relations, the following recurrence formula about P_m^0 is derived,

$$P_m^0 + P_{m-1}^0 + \left[1 - 3\alpha(1-\alpha)\right] P_{m-2}^0 = 1 - \alpha(1-\alpha). \tag{7.33}$$

The solution of Eq. (7.33) for the initial values of $P_0^0 = 1$, $P_1^0 = 0$ is given by

$$P_m^0 = \frac{1}{3} + \frac{1}{3}\left[-\frac{1}{2} + \frac{\sqrt{3}(1-2\alpha)i}{2}\right]^m + \frac{1}{3}\left[-\frac{1}{2} - \frac{\sqrt{3}(1-2\alpha)i}{2}\right]^m, \tag{7.34}$$

and it can be rewritten as

$$P_m^0 = \frac{1}{3} + \frac{2}{3}\left[-\sqrt{1-3\alpha(1-\alpha)}\right]^m \cos\left\{m \arctan\left[\sqrt{3}(1-2\alpha)\right]\right\}. \tag{7.35}$$

The substitution: $\theta = \arctan\left[\sqrt{3}(1-2\alpha)\right]$ for Eqs. (7.34) and (7.35) gives

$$P_m^0 = \frac{1}{3} + \frac{1}{3}\left[-\sqrt{1-3\alpha(1-\alpha)}\right]^m \left(e^{im\theta} + e^{-im\theta}\right)$$

$$= \frac{1}{3} + \frac{2}{3}\left[-\sqrt{1-3\alpha(1-\alpha)}\right]^m \cos(m\theta), \tag{7.36}$$

and also the relations :

$$P_m^+ = \frac{1}{3} - \frac{1}{3}\left[-\sqrt{1-3\alpha(1-\alpha)}\right]^m\left(\frac{1-\sqrt{3}\,i}{2}e^{im\theta} + \frac{1+\sqrt{3}\,i}{2}e^{-im\theta}\right)$$

$$= \frac{1}{3} - \frac{1}{3}\left[-\sqrt{1-3\alpha(1-\alpha)}\right]^m\left[\cos(m\theta) + \sqrt{3}\sin(m\theta)\right], \tag{7.37}$$

$$P_m^- = \frac{1}{3} - \frac{1}{3}\left[-\sqrt{1-3\alpha(1-\alpha)}\right]^m\left(\frac{1+\sqrt{3}\,i}{2}e^{im\theta} + \frac{1-\sqrt{3}\,i}{2}e^{-im\theta}\right)$$

$$= \frac{1}{3} - \frac{1}{3}\left[-\sqrt{1-3\alpha(1-\alpha)}\right]^m\left[\cos(m\theta) - \sqrt{3}\sin(m\theta)\right], \tag{7.38}$$

and the following relations:

$$P_{-m}^0 = P_m^0 \tag{7.39}$$

$$P_{-m}^+ = P_m^- \tag{7.40}$$

$$P_{-m}^- = P_m^+ \tag{7.41}$$

are also satisfied.

For the case of $h'-k'=3N$ (N : integer), Eq. (7.29) :

$$\langle J_m(\vec{K})\rangle = \left|F_0(\vec{K})\right|^2\left[P_m^0 + P_m^+ e^{-2\pi i(h'-k')/3} + P_m^- e^{2\pi i(h'-k')/3}\right]$$

is reduced to $\langle J_m(\vec{K})\rangle = \left|F_0(\vec{K})\right|^2$. Furthermore, the intensity given by Eq. (7.23) :

$$I(h',k',l') = \sum_{m=-\infty}^{\infty} J_m(h',k',l')e^{2\pi iml'} ,$$

or

$$I(h',k',l_{\mathrm{H}}) = \sum_{m=-\infty}^{\infty} J_m(h',k',l_{\mathrm{H}})e^{2\pi iml_{\mathrm{H}}/3} , \tag{7.42}$$

has non-zero values only for the case $l'=N'$ or $l_{\mathrm{H}} = 3l' = 3N'$ (N' : integer), and becomes zero otherwise. It means that a sharp diffraction peak should appear in the case $l_{\mathrm{H}} = 3l' = 3N'$, for arbitrary values of α , no matter there should be any stacking faults. It appears to be reasonable because the interplaner spacing of the (111)-lattice plane is not affected by the fault in stacking of the (111) plane.

For the case of $h'-k'=3N\pm1$, by applying Eq. (7.29) :

$$\langle J_m(\vec{K})\rangle = \left|F_0(\vec{K})\right|^2\left(P_m^0 + P_m^+ e^{\mp 2\pi i/3} + P_m^- e^{\pm 2\pi i/3}\right)$$

to Eq. (7.42), the formula of the diffraction intensity is given by

$$I(h',k',l_{\mathrm{H}}) = \left|F_0(\vec{K})\right|^2\sum_{m=-\infty}^{\infty}\left(P_m^0 + P_m^+ e^{\mp 2\pi i/3} + P_m^- e^{\pm 2\pi i/3}\right)e^{2\pi iml_{\mathrm{H}}/3}$$

$$= \left|F_0(\vec{K})\right|^2\left[1 + \sum_{m=-\infty}^{-1}\left(P_m^0 + P_m^+ e^{\mp 2\pi i/3} + P_m^- e^{\pm 2\pi i/3}\right)e^{2\pi iml_{\mathrm{H}}/3}\right.$$

$$+\sum_{m=1}^{\infty}\left(P_m^0 + P_m^+ \, e^{\mp 2\pi i/3} + P_m^- \, e^{\pm 2\pi i/3}\right)e^{2\pi i ml_{\mathrm{H}}/3}\Bigg]$$

$$=\left|F_0(\vec{K})\right|^2 \Bigg[1+\sum_{m=1}^{\infty}\left(P_m^0 + P_m^- \, e^{\mp 2\pi i/3} + P_m^+ \, e^{\pm 2\pi i/3}\right)e^{-2\pi i ml_{\mathrm{H}}/3}$$

$$+\sum_{m=1}^{\infty}\left(P_m^0 + P_m^+ \, e^{\mp 2\pi i/3} + P_m^- \, e^{\pm 2\pi i/3}\right)e^{2\pi i ml_{\mathrm{H}}/3}\Bigg]$$

$$=\left|F_0(\vec{K})\right|^2 \Bigg[1+\sum_{m=1}^{\infty} P_m^0\left(e^{2\pi i ml_{\mathrm{H}}/3}+e^{-2\pi i ml_{\mathrm{H}}/3}\right)+\sum_{m=1}^{\infty} P_m^+\left(e^{2\pi i(ml_{\mathrm{H}}\mp 1)/3}+e^{-2\pi i(ml_{\mathrm{H}}\mp 1)/3}\right)$$

$$+\sum_{m=1}^{\infty} P_m^-\left(e^{2\pi i(ml_{\mathrm{H}}\pm 1)/3}+e^{-2\pi i(ml_{\mathrm{H}}\pm 1)/3}\right)\Bigg]$$

$$=\left|F_0(\vec{K})\right|^2 \Bigg[1+2\sum_{m=1}^{\infty} P_m^0 \cos\frac{2\pi ml_{\mathrm{H}}}{3}+2\sum_{m=1}^{\infty} P_m^+ \cos\frac{2\pi(ml_{\mathrm{H}}\mp 1)}{3}$$

$$+2\sum_{m=1}^{\infty} P_m^- \cos\frac{2\pi(ml_{\mathrm{H}}\pm 1)}{3}\Bigg],$$

and the application of Eqs. (7.36), (7.37), (7.38) :

$$P_m^0 = \frac{1}{3}+\frac{2}{3}\left[-\sqrt{1-3\alpha(1-\alpha)}\,\right]^m \cos(m\theta)$$

$$P_m^+ = \frac{1}{3}-\frac{1}{3}\left[-\sqrt{1-3\alpha(1-\alpha)}\,\right]^m \left[\cos(m\theta)+\sqrt{3}\sin(m\theta)\right]$$

$$P_m^- = \frac{1}{3}-\frac{1}{3}\left[-\sqrt{1-3\alpha(1-\alpha)}\,\right]^m \left[\cos(m\theta)-\sqrt{3}\sin(m\theta)\right]$$

will give

$$=\left|F_0(\vec{K})\right|^2 \Bigg(1+2\sum_{m=1}^{\infty}\left\{\frac{1}{3}+\frac{2}{3}\left[-\sqrt{1-3\alpha(1-\alpha)}\,\right]^m \cos(m\theta)\right\}\cos\frac{2\pi ml_{\mathrm{H}}}{3}$$

$$+2\sum_{m=1}^{\infty}\left\{\frac{1}{3}-\frac{1}{3}\left[-\sqrt{1-3\alpha(1-\alpha)}\,\right]^m \left[\cos(m\theta)+\sqrt{3}\sin(m\theta)\right]\right\}$$

$$\times\cos\frac{2\pi(ml_{\mathrm{H}}\mp 1)}{3}$$

$$+2\sum_{m=1}^{\infty}\left\{\frac{1}{3}-\frac{1}{3}\left[-\sqrt{1-3\alpha(1-\alpha)}\,\right]^m \left[\cos(m\theta)-\sqrt{3}\sin(m\theta)\right]\right\}$$

$$\times\cos\frac{2\pi(ml_{\mathrm{H}}\pm 1)}{3}\Bigg)$$

$$=\left|F_0(\vec{K})\right|^2 \Bigg(1+2\sum_{m=1}^{\infty}\left\{\frac{1}{3}+\frac{2}{3}\left[-\sqrt{1-3\alpha(1-\alpha)}\,\right]^m \cos(m\theta)\right\}\cos\frac{2\pi ml_{\mathrm{H}}}{3}$$

$$+2\sum_{m=1}^{\infty}\left\{\frac{1}{3}-\frac{1}{3}\left[-\sqrt{1-3\alpha(1-\alpha)}\,\right]^m \left[\cos(m\theta)+\sqrt{3}\sin(m\theta)\right]\right\}$$

$$\times\left(\cos\frac{2\pi ml_{\mathrm{H}}}{3}\cos\frac{2\pi}{3}\pm\sin\frac{2\pi ml_{\mathrm{H}}}{3}\sin\frac{2\pi}{3}\right)$$

$$+2\sum_{m=1}^{\infty}\left\{\frac{1}{3}-\frac{1}{3}\left[-\sqrt{1-3\alpha(1-\alpha)}\right]^{m}\left[\cos(m\theta)-\sqrt{3}\sin(m\theta)\right]\right\}$$

$$\times\left(\cos\frac{2\pi ml_{\mathrm{H}}}{3}\cos\frac{2\pi}{3}\mp\sin\frac{2\pi ml_{\mathrm{H}}}{3}\sin\frac{2\pi}{3}\right)\Bigg)$$

$$=\left|F_{0}(\vec{K})\right|^{2}\Bigg(1+2\sum_{m=1}^{\infty}\left\{\frac{1}{3}+\frac{2}{3}\left[-\sqrt{1-3\alpha(1-\alpha)}\right]^{m}\cos(m\theta)\right\}\cos\frac{2\pi ml_{\mathrm{H}}}{3}$$

$$+2\sum_{m=1}^{\infty}\left\{\frac{1}{3}-\frac{1}{3}\left[-\sqrt{1-3\alpha(1-\alpha)}\right]^{m}\left[\cos(m\theta)+\sqrt{3}\sin(m\theta)\right]\right\}$$

$$\times\left(-\frac{1}{2}\cos\frac{2\pi ml_{\mathrm{H}}}{3}\pm\frac{\sqrt{3}}{2}\sin\frac{2\pi ml_{\mathrm{H}}}{3}\right)$$

$$+2\sum_{m=1}^{\infty}\left\{\frac{1}{3}-\frac{1}{3}\left[-\sqrt{1-3\alpha(1-\alpha)}\right]^{m}\left[\cos(m\theta)-\sqrt{3}\sin(m\theta)\right]\right\}$$

$$\times\left(-\frac{1}{2}\cos\frac{2\pi ml_{\mathrm{H}}}{3}\mp\frac{\sqrt{3}}{2}\sin\frac{2\pi ml_{\mathrm{H}}}{3}\right)\Bigg).$$

When we express the above equation by the following formula,

$$I(h',k',l_{\mathrm{H}})=C\sum_{n=0}^{\infty}\left[a_{n}\cos\left(\frac{2\pi nl_{\mathrm{H}}}{3}\right)+b_{n}\sin\left(\frac{2\pi nl_{\mathrm{H}}}{3}\right)\right],\tag{7.42}$$

we find the following relations,

$$a_{0}=1,\tag{7.43}$$

$$a_{n}=2\left\{\frac{1}{3}+\frac{2}{3}\left[-\sqrt{1-3\alpha(1-\alpha)}\right]^{n}\cos(n\theta)\right\}$$

$$-\left\{\frac{1}{3}-\frac{1}{3}\left[-\sqrt{1-3\alpha(1-\alpha)}\right]^{n}\left[\cos(n\theta)+\sqrt{3}\sin(n\theta)\right]\right\}$$

$$-\left\{\frac{1}{3}-\frac{1}{3}\left[-\sqrt{1-3\alpha(1-\alpha)}\right]^{n}\left[\cos(n\theta)-\sqrt{3}\sin(n\theta)\right]\right\}$$

$$=2\left[-\sqrt{1-3\alpha(1-\alpha)}\right]^{n}\cos(n\theta)\qquad\left[n\neq0\right],\tag{7.44}$$

$$b_{0}=0,\tag{7.45}$$

$$b_{n}=\pm\sqrt{3}\left\{\frac{1}{3}-\frac{1}{3}\left[-\sqrt{1-3\alpha(1-\alpha)}\right]^{n}\left[\cos(n\theta)+\sqrt{3}\sin(n\theta)\right]\right\}$$

$$\mp\sqrt{3}\left\{\frac{1}{3}-\frac{1}{3}\left[-\sqrt{1-3\alpha(1-\alpha)}\right]^{n}\left[\cos(n\theta)-\sqrt{3}\sin(n\theta)\right]\right\}$$

$$=\mp2\left[-\sqrt{1-3\alpha(1-\alpha)}\right]^{n}\sin(n\theta)\qquad\left[n\neq0\right],\tag{7.46}$$

where the double sign: $\pm$ is corresponded to $h' - k' = 3N \pm 1$.

Eq. (7.42) can be further modified as

$$I(h',k',l_H) = C\left\{1 + 2\sum_{n=1}^{\infty}\left[-\sqrt{1-3\alpha(1-\alpha)}\right]^n\left[\cos(n\theta)\cos\left(\frac{2\pi nl_H}{3}\right) \mp \sin(n\theta)\sin\left(\frac{2\pi nl_H}{3}\right)\right]\right\}$$

$$= C\left\{1 + 2\sum_{n=1}^{\infty}\left[-\sqrt{1-3\alpha(1-\alpha)}\right]^n\cos\left(\frac{2\pi nl_H}{3} \pm n\theta\right)\right\}$$

$$= C\left\{1 + 2\sum_{n=1}^{\infty}\left[\sqrt{1-3\alpha(1-\alpha)}\right]^n\cos\left(\frac{2\pi nl_H}{3} \pm n\theta + n\pi\right)\right\}$$

$$= C\left\{1 + 2\sum_{n=1}^{\infty}\left[\sqrt{1-3\alpha(1-\alpha)}\right]^n\cos\left[2\pi n\left(\frac{l_H}{3} + \frac{1}{2} \pm \frac{\theta}{2\pi}\right)\right]\right\}. \tag{7.47}$$

Since the following relation generally holds,

$$1 + 2\sum_{n=1}^{\infty}r^n\cos(n\theta) = -1 + \sum_{n=0}^{\infty}r^n\left(e^{in\theta} + e^{-in\theta}\right)$$

$$= -1 + \frac{1}{1-re^{i\theta}} + \frac{1}{1-re^{-i\theta}} = \frac{-\left(1-re^{i\theta}\right)\left(1-re^{-i\theta}\right) + 1 - re^{-i\theta} + 1 - re^{i\theta}}{\left(1-re^{i\theta}\right)\left(1-re^{-i\theta}\right)}$$

$$= \frac{-\left(1-re^{i\theta}-re^{-i\theta}+r^2\right) + 1 - re^{-i\theta} + 1 - re^{i\theta}}{1-re^{i\theta}-re^{-i\theta}+r^2} = \frac{1-r^2}{1+r^2-2\cos\theta},$$

the sum of Eq. (7.47) for $\alpha \neq 0,1$ will give the formula :

$$I(h',k',l_H) = C\frac{1-\left[1-3\alpha(1-\alpha)\right]}{1+\left[1-3\alpha(1-\alpha)\right] - 2\sqrt{1-3\alpha(1-\alpha)}\cos\left[2\pi\left(\frac{l_H}{3} + \frac{1}{2} \pm \frac{\theta}{2\pi}\right)\right]}$$

$$= C\frac{\frac{3}{2}\alpha(1-\alpha)}{1 - \frac{3}{2}\alpha(1-\alpha) - \sqrt{1-3\alpha(1-\alpha)}\cos\left[2\pi\left(\frac{l_H}{3} + \frac{1}{2} \pm \frac{\theta}{2\pi}\right)\right]}. \tag{7.48}$$

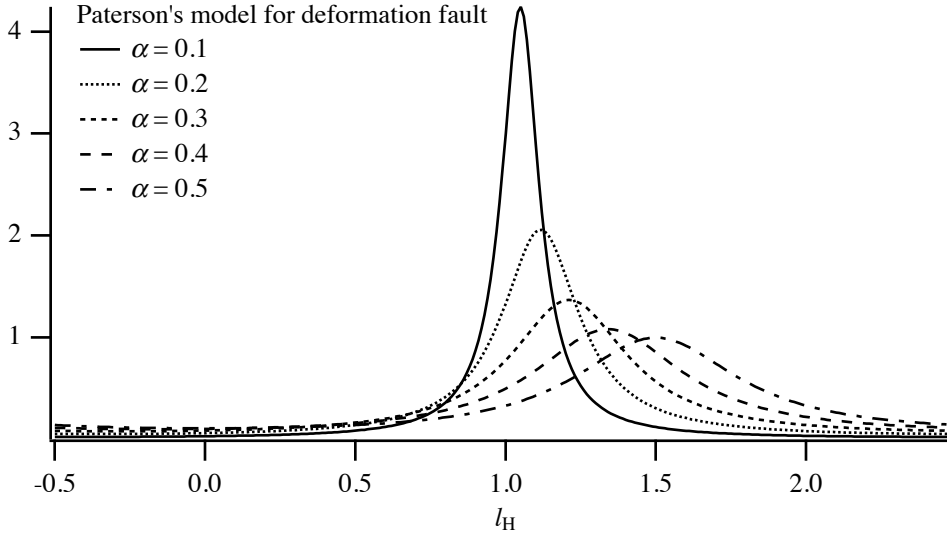Figure 7.6 illustrates the intensity distribution given by Eq. (7.48).

Fig. 7.6 Diffraction peak profile for deformation fault based on the Paterson's theory, in the case of $h' - k' = 1$.

We can find that the location of the peak is shifted and broadened on larger value of the frequency of stacking fault α. The peak location for $h' - k' = 3N \pm 1$ is given by $\dfrac{l_{\mathrm{H}}}{3} + \dfrac{1}{2} \pm \dfrac{\theta}{2\pi} = N'$ (N': integer), that is, the position of the peak is given by

$$l_{\mathrm{H}} = 3N' - \frac{3}{2} \mp \frac{3}{2\pi} \arctan\left[\sqrt{3}(1 - 2\alpha) \right].$$
(7.49)

As the peak location for $\alpha = 0$ is given by $\arctan\left[\sqrt{3}(1 - 2\alpha) \right] = \dfrac{\pi}{3}$, the original (non-shifted) peak position for $h' - k' = 3N \pm 1$ should be given by $l_{\mathrm{H}} = 3N' - \dfrac{3}{2} \mp \dfrac{1}{2} = \left\{ \begin{array}{l} 3N' - 2 \\ 3N' - 1 \end{array} \right.$.

Here we introduce
$$y = \arctan x ,$$
and the following relation :
$$\frac{\mathrm{d}\,y}{\mathrm{d}\,x} = \frac{1}{1 + x^2} ,$$
gives
$$\frac{\mathrm{d}}{\mathrm{d}\alpha} \arctan\left[\sqrt{3}(1 - 2\alpha) \right] = -\frac{2\sqrt{3}}{1 + 3(1 - 2\alpha)^2} ,$$
and then
$$\arctan\left[\sqrt{3}(1 - 2\alpha) \right] \sim \frac{\pi}{3} - \frac{\sqrt{3}\alpha}{2} .$$
The peak location is approximated by
$$l_{\mathrm{H}} = 3N' - \frac{3}{2} \mp \frac{3}{2\pi} \arctan\left[\sqrt{3}(1 - 2\alpha) \right]$$

$$\sim 3N' - \frac{3}{2} \mp \left(\frac{1}{2} - \frac{3\sqrt{3}\alpha}{4\pi} \right),$$

and the shift of the peak is given by

$$\Delta l_{\mathrm{H}} = 3N' - \frac{3}{2} \mp \frac{3}{2\pi} \arctan\left[\sqrt{3}(1-2\alpha) \right] - \left(3N' - \frac{3}{2} \mp \frac{1}{2} \right)$$

$$= \pm \frac{1}{2} \mp \frac{3}{2\pi} \arctan\left[\sqrt{3}(1-2\alpha) \right]$$

$$\sim \pm \frac{3\sqrt{3}\alpha}{4\pi} \,.$$

Next, let us evaluate the approximate value for the broadening. The integrated intensity of one diffraction peak should be given by $\displaystyle\int_{\mathrm{peak}\,l_{\mathrm{H}}-3/2}^{\mathrm{peak}\,l_{\mathrm{H}}+3/2} I(h',k',l_{\mathrm{H}})\mathrm{d}l_{\mathrm{H}}$, and from Eq. (7.47), the intensity

profile should be given by

$$I(h',k',l_{\mathrm{H}}) = C\left\{ 1 + 2\sum_{n=1}^{\infty} \left[\sqrt{1-3\alpha(1-\alpha)} \right]^{n} \cos\left[2\pi n\left(\frac{l_{\mathrm{H}}}{3} + \frac{1}{2} \pm \frac{\theta}{2\pi} \right) \right] \right\},$$

and then, we obtain

$$\int_{\mathrm{peak}\,l_{\mathrm{H}}-3/2}^{\mathrm{peak}\,l_{\mathrm{H}}+3/2} I(h',k',l_{\mathrm{H}})\mathrm{d}l_{\mathrm{H}} = C\int_{-3/2}^{3/2} \left\{ 1 + 2\sum_{n=1}^{\infty} \left[\sqrt{1-3\alpha(1-\alpha)} \right]^{n} \cos\frac{2\pi nl}{3} \right\}\mathrm{d}l$$

$$= C\left\{ 3 + 2\sum_{n=1}^{\infty} \left[\sqrt{1-3\alpha(1-\alpha)} \right]^{n} \int_{-3/2}^{3/2} \cos\frac{2\pi nl}{3}\mathrm{d}l \right\}$$

$$= C\left\{ 3 + 2\sum_{n=1}^{\infty} \left[\sqrt{1-3\alpha(1-\alpha)} \right]^{n} \left[\frac{3}{2\pi n}\sin\frac{2\pi nl}{3} \right]_{-3/2}^{3/2} \right\}$$

$$= 3C \,.$$

As the value of the peak-top intensity is given by

$$I_{\max}(h',k',l_{\mathrm{H}}) = C\frac{\dfrac{3}{2}\alpha(1-\alpha)}{1 - \dfrac{3}{2}\alpha(1-\alpha) - \sqrt{1-3\alpha(1-\alpha)}} \,,$$

the integral breadth β_{H} is given by the following equation,

$$\beta_{\mathrm{H}} = \frac{\displaystyle\int_{\mathrm{peak}\,l_{\mathrm{H}}-3/2}^{\mathrm{peak}\,l_{\mathrm{H}}+3/2} I(h',k',l_{\mathrm{H}})\mathrm{d}l_{\mathrm{H}}}{I_{\max}(h',k',l_{\mathrm{H}})} \tag{7.50}$$

$$= \frac{3\left[1 - \dfrac{3}{2}\alpha(1-\alpha) - \sqrt{1-3\alpha(1-\alpha)} \right]}{\dfrac{3}{2}\alpha(1-\alpha)} = \frac{3\left[2 - 3\alpha(1-\alpha) - 2\sqrt{1-3\alpha(1-\alpha)} \right]}{3\alpha(1-\alpha)}$$

$$= \frac{3\left[1-\sqrt{1-3\alpha(1-\alpha)}\right]^2}{\left[1-\sqrt{1-3\alpha(1-\alpha)}\right]\left[1+\sqrt{1-3\alpha(1-\alpha)}\right]}$$

$$= \frac{3\left[1-\sqrt{1-3\alpha(1-\alpha)}\right]}{1+\sqrt{1-3\alpha(1-\alpha)}}$$

$$\sim \frac{9\alpha}{4} .$$

(7.51)

7-2-2 Powder diffraction pattern

In powder diffraction measurements, diffractions from different lattice planes may appear at the same position, when the diffraction angles have the same value. For example, the $\{111\}$-peak for a cubic crystal system consists of 111, $11\bar{1}$, $1\bar{1}1$, $\bar{1}11$, $\bar{1}\bar{1}\bar{1}$, $\bar{1}\bar{1}1$, $\bar{1}1\bar{1}$, and $1\bar{1}\bar{1}$-reflections. The group of reflections symmetrically equivalent is called the **equivalent reflections**, but they generally become non-equivalent when there exists a stacking fault.

In the former section, the diffraction peak profile was expressed by the hexagonal index $h'k'l_{\mathrm{H}}$, and the expression with the cubic index hkl will be derived in the following. The relations between the lattice vectors $\vec{a}$, $\vec{b}$, $\vec{c}$, $\vec{a}'$, $\vec{b}'$, $\vec{c}_{\mathrm{H}}$ and the corresponding reciprocal lattice vectors are summarized as follows,

$$\vec{a}' = \frac{-\vec{a}+\vec{b}}{2} ,$$

$$\vec{b}' = \frac{-\vec{b}+\vec{c}}{2} ,$$

$$\vec{c}_{\mathrm{H}} = \vec{a}+\vec{b}+\vec{c} ,$$

$$\vec{a}'^* = \frac{2\left(-2\vec{a}+\vec{b}+\vec{c}\right)}{3a^2} = -\frac{4}{3}\vec{a}^* +\frac{2}{3}\vec{b}^* +\frac{2}{3}\vec{c}^* ,$$

$$\vec{b}'^* = \frac{2\left(-\vec{a}-\vec{b}+2\vec{c}\right)}{3a^2} = -\frac{2}{3}\vec{a}^* -\frac{2}{3}\vec{b}^* +\frac{4}{3}\vec{c}^* ,$$

$$\vec{c}_{\mathrm{H}}^* = \frac{\vec{a}+\vec{b}+\vec{c}}{3a^2} = \frac{1}{3}\vec{a}^* +\frac{1}{3}\vec{b}^* +\frac{1}{3}\vec{c}^* .$$

In order to derive the relations between the cubic index hkl and the hexagonal index $h'k'l_{\mathrm{H}}$, the relation : $\vec{K} = h'\vec{a}'^* + k'\vec{b}'^* + l_{\mathrm{H}}\vec{c}_{\mathrm{H}}^* = h\vec{a}^* + k\vec{b}^* + l\vec{c}^*$ is applied as follows,

$$h' = \vec{K}\cdot\vec{a}' = \frac{-h+k}{2} ,$$

$$k' = \vec{K}\cdot\vec{b}' = \frac{-k+l}{2} ,$$

$$l_{\mathrm{H}} = \vec{K}\cdot\vec{c}_{\mathrm{H}} = h+k+l ,$$

$$h = \vec{K} \cdot \vec{a} = \frac{-4h' - 2k' + l_{\mathrm{H}}}{3},$$

$$k = \vec{K} \cdot \vec{b} = \frac{2h' - 2k' + l_{\mathrm{H}}}{3},$$

$$l = \vec{K} \cdot \vec{c} = \frac{2h' + 4k' + l_{\mathrm{H}}}{3}.$$

Then we obtain

$$h' - k' = \frac{-h + 2k - l}{2},$$

and

$$l_{\mathrm{H}} = h + k + l.$$

For example, the index for the cubic system $1\bar{1}1$ will give $h' - k' = -2$, $l_{\mathrm{H}} = 1$.

Since $-l_{\mathrm{H}} = 3N \mp 1$ is equivalent to $l_{\mathrm{H}} = 3N \pm 1$ for the behavior about approaching to $l_{\mathrm{H}} = 0$ or departing from $l_{\mathrm{H}} = 0$, the shift of the powder diffraction peak can be described by the absolute value of the index, $|l_{\mathrm{H}}| = |h + k + l|$. The diffraction peak for the case: "the absolute value of the sum of the Miller's indices for the cubic system" is a multiple of 3, that is, $|h + k + l| = 3N$, should have sharp and unshifted profile, and it should be broadened and shifted to higher diffraction angles for the case $|h + k + l| = 3N + 1$, and it should also be broadened but shifted to lower diffraction angles fo the case $|h + k + l| = 3N - 1$. The 111 and $\bar{1}\bar{1}\bar{1}$-reflections remains sharp because $|h + k + l| = 3N$, but the $11\bar{1}$, $1\bar{1}1$, $\bar{1}11$, $\bar{1}\bar{1}1$, $\bar{1}1\bar{1}$ and $1\bar{1}\bar{1}$-reflections are shifted to higher angle side and broadened, because $|h + k + l| = 3N + 1$.

In usual powder diffraction measurements, the diffraction intensity profile is recorded for the diffraction angle 2θ, or the length of the scattering vector (d^*-value), $d^* = K = \frac{2\sin\theta}{\lambda}$. How the peak-shift and broadening are expressed in the profile plotted for the values of 2θ or d^*?

It is better to clarify the formula for the three-dimensional diffraction peak intensity distribution from a small single crystallite as a function of variable scattering vector, to solve this problem, even if it may technically difficult to be observed. The diffraction intensity from a hypothetical perfect crystal appears only when the scattering vector matches to one of the reciprocal lattice points, the diffraction intensity distribution will appear as a sharp spot in the reciprocal space. When a stacking fault exists, the diffraction spot should be shifted from a reciprocal lattice point and broadened, and both the shift and broadening should occur only along the direction of $\vec{c}_{\mathrm{H}}^*$.
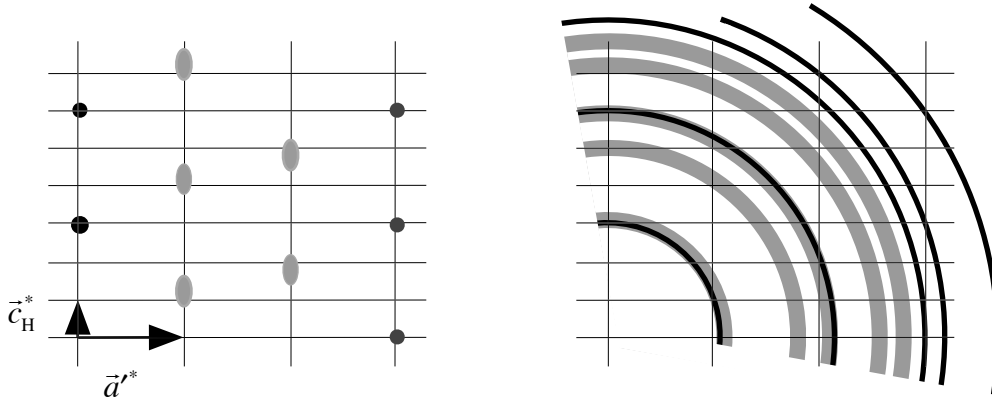
Fig. 7.7 The diffraction spots (left) and powder diffraction pattern (right) affected by stacking falt .

The powder diffraction intensity profile affected by the stacking fault should be given by the radial distribution of the onion-like trace of the deformed diffraction spots, rotated around the origin. Figure 7.7 illustrates the diffraction spots and the corresponding powder diffraction intensity profile. Powder diffraction intensity profile can be evaluated as the projection of diffraction spots deformed along $\vec{c}_{H}^{*}$ -direction onto the radial direction.

The peak shift along the $\vec{c}_{H}^{*}$ -direction is given by

$$\left(\Delta l_{H}\right)\vec{c}_{H}^{*} = \pm\left\{\frac{1}{2} - \frac{3}{2\pi}\arctan\left[\sqrt{3}(1-2\alpha)\right]\right\}\vec{c}_{H}^{*} ,$$

for $\left|h+k+l\right| = 3N \pm 1$, and the projection along the direction :

$$\vec{K} = h\vec{a}^{*} + k\vec{b}^{*} + l\vec{c}^{*}$$

is derived from the relation :

$$\vec{c}_{H}^{*} = \frac{\vec{a}+\vec{b}+\vec{c}}{3a^{2}} = \frac{1}{3}\vec{a}^{*} + \frac{1}{3}\vec{b}^{*} + \frac{1}{3}\vec{c}^{*}$$

as follows,

$$d_{peak}^{*} - d_{hkl}^{*} = \left(\Delta l_{H}\right)\vec{c}_{H}^{*} \cdot \frac{\vec{K}}{K}$$

$$= \pm\left\{\frac{1}{2} - \frac{3}{2\pi}\arctan\left[\sqrt{3}(1-2\alpha)\right]\right\}\vec{c}_{H}^{*} \cdot \frac{\vec{K}}{K}$$

$$= \frac{\pm\left|h+k+l\right|}{3\sqrt{h^{2}+k^{2}+l^{2}}\,a}\left\{\frac{1}{2} - \frac{3}{2\pi}\arctan\left[\sqrt{3}(1-2\alpha)\right]\right\}$$

$$\sim \frac{\pm\sqrt{3}\left|h+k+l\right|\alpha}{4\pi\sqrt{h^{2}+k^{2}+l^{2}}\,a}$$

The peak shift on the horizontal axis of the diffraction angle 2θ is evaluated by applying the relations : $d^{*} = \frac{2\sin\theta}{\lambda}$ and $\Delta d^{*} = \frac{(\Delta 2\theta)\cos\theta}{\lambda} = \frac{(\Delta 2\theta)d^{*}}{2\tan\theta}$, as follows,

$$2\theta_{peak} - 2\theta_{hkl} = \frac{2\left(d_{peak}^{*} - d_{hkl}^{*}\right)\tan\theta}{d^{*}}$$

$$= \frac{\pm 2|h+k+l|\tan\theta}{3(h^2+k^2+l^2)}\left\{\frac{1}{2}-\frac{3}{2\pi}\arctan\left[\sqrt{3}(1-2\alpha)\right]\right\}$$

$$\sim \frac{\pm\sqrt{3}\alpha|h+k+l|\tan\theta}{2\pi(h^2+k^2+l^2)} .$$

The integral breadth is similarly evaluated as follows. As the integral breadth along the $\vec{c}_H^*$-direction is given by

$$\beta_H\vec{c}_H^* = \frac{3\left[1-\sqrt{1-3\alpha(1-\alpha)}\right]}{1+\sqrt{1-3\alpha(1-\alpha)}}\vec{c}_H^* ,$$

the breadth is given in the wavenumber expression by

$$\Delta d^* = \beta_H\vec{c}_H^* \cdot \frac{\vec{K}}{K}$$

$$= \frac{3\left[1-\sqrt{1-3\alpha(1-\alpha)}\right]}{1+\sqrt{1-3\alpha(1-\alpha)}}\vec{c}_H^* \cdot \frac{\vec{K}}{K}$$

$$= \frac{\left[1-\sqrt{1-3\alpha(1-\alpha)}\right]|h+k+l|}{\left[1+\sqrt{1-3\alpha(1-\alpha)}\right]\sqrt{h^2+k^2+l^2}\,a}$$

$$\sim \frac{3\alpha|h+k+l|}{4\sqrt{h^2+k^2+l^2}\,a} ,$$

and given in the diffraction-angle expression by

$$\Delta 2\theta = \frac{2\Delta d^* \tan\theta}{d^*}$$

$$= \frac{2\left[1-\sqrt{1-3\alpha(1-\alpha)}\right]|h+k+l|\tan\theta}{\left[1+\sqrt{1-3\alpha(1-\alpha)}\right](h^2+k^2+l^2)}$$

$$\sim \frac{3\alpha|h+k+l|\tan\theta}{2(h^2+k^2+l^2)} .$$

Figure 7.8 summarize the diffraction pattern affected by the deformation fault of the stacking along the (111)-direction of a cubic close packing structure.

The {111}-reflection peak is the overlap of the sharp 111 and $\overline{1}\,\overline{1}\,\overline{1}$ peaks ($|h+k+l|$ is a

multiple of 3) and broad $11\overline{1}$, $1\overline{1}1$, $\overline{1}11$, $\overline{1}\,\overline{1}1$, $\overline{1}1\overline{1}$, $1\overline{1}\,\overline{1}$ peaks shifted to the higher angle side (remainder 1 on division of $|h+k+l|$ by 3). So the observed {111}-diffraction profile should be "an asymmetric profile, slightly shifted to higher angle side, having sharp peak-top and long tails".

The {200}-reflection is composed of 200, $\overline{2}00$, 020, $0\overline{2}0$, 002, $00\overline{2}$ reflections, and all the components belong to the same class of remainder 2 on division of $|h+k+l|$ by 3. As all the

components are broadened and shifted to lower angle side, the observed powder diffraction peak profile should be broad and shifted to the lower angle side.

As the {220}-reflection is the overlap of sharp $2\bar{2}0$ -type component ($\left|h+k+l\right|$ is a multiple of 3) and broad 220 -type component shifted toward the higher angle side (remainder 1 on division of $\left|h+k+l\right|$ by 3), the observed peak profile should have sharp peak-top and long tails slightly shifted to the higher angle side, similarly to the {111}-reflection. But the deformation of the {220}-peak profile should slightly be different from the {111}-peak, because the ratio of the intensities of the sharp $20\bar{2}$, $2\bar{2}0$, $02\bar{2}$, $02\bar{2}$, $0\bar{2}2$, $\bar{2}20$, $\bar{2}02$ -reflections to the broad 220 , 202 , 022 , $0\bar{2}2$, $\bar{2}0\bar{2}$, $\bar{2}\bar{2}0$ - reflections is 1:1, while that of the sharp 111 , $\bar{1}\bar{1}\bar{1}$ -reflections to the broad $11\bar{1}$, $1\bar{1}1$, $1\bar{1}\bar{1}$, $\bar{1}11$, $\bar{1}1\bar{1}$, $\bar{1}\bar{1}1$-reflections is 1:3, and the amount of broadening and peak shift are also different.

The {311}-reflection will be the overlap of the sharp $31\bar{1}$ -type component ($\left|h+k+l\right|$ is a multiple of 3), broad -type component (remainder 1 on division of $\left|h+k+l\right|$ by 3) shifted to the higher angle side, and another broad 311-type component (remainder 2 on division of $\left|h+k+l\right|$ by 3) shifted to the lower angle side.
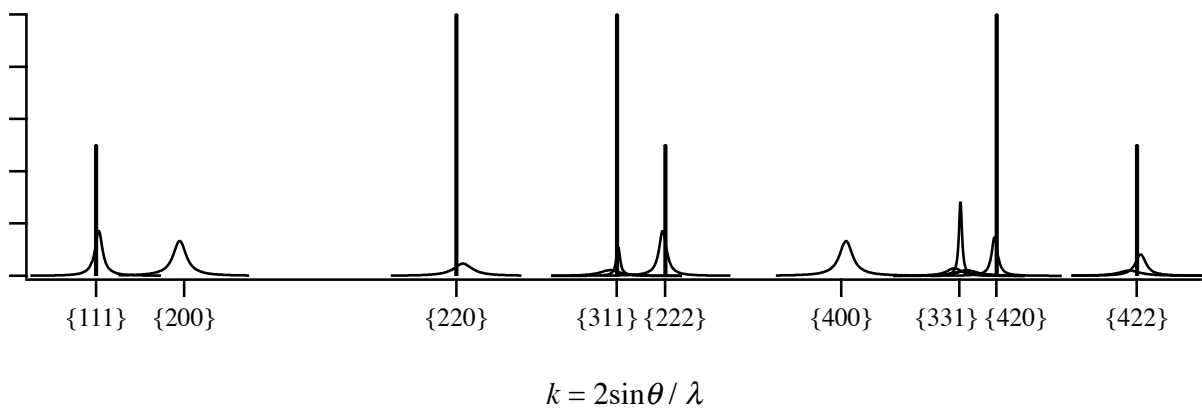

$$k = 2\sin\theta / \lambda$$

Fig. 7.8 Broadening and shift of powder diffraction peak profile for deformation fault in stacking along (111) direction of a cubic close packing structure.